(NASA-CR-124254) PARTICLE-FLUID INTERACTION CORRECTIONS FOR FLOW MEASUREMENTS WITH A LASER DOPPLER FLOWMETER (Arizona State Univ.) 61 p HC $5.25 CSCL 14B G3/12

N73-23379

Unclas 03846

Engineering Research Center

College of Engineering Sciences
Arizona State University
Tempe, Ariz. 85281

N73-23379

PARTICLE-FLUID INTERACTION CORRECTIONS FOR FLOW MEASUREMENTS WITH A LASER DOPPLER FLOWMETER

by

Neil S. Berman

Prepared under Contract No. NAS 8-21397

National Aeronautics and Space Administration
George C. Marshall Space Flight Center
Aero-Astrodynamics Laboratory
Aerophysics Division
Thermal Environment Branch
Physics Section

ENGINEERING RESEARCH CENTER

COLLEGE OF ENGINEERING SCIENCES

ARIZONA STATE UNIVERSITY

TEMPE, ARIZONA 85281

TABLE OF CONTENTS

ABSTRACT

A discussion is given of particle lags in mean flows, acoustic oscillations at single frequencies and in turbulent flows. Some simplified cases lead to exact solutions. For turbulent flows linearization of the equation of motion after assuming the fluid and particle streamlines coincide also leads to a solution. The results show that particle lags are a function of particle size and frequency of oscillation. Additional studies are necessary to evaluate the effect of turbulence when a major portion of the energy is concentrated in small eddies.

INTRODUCTION

A promising method of measuring turbulent flow characteristics is the Laser-Doppler technique. Local mean and fluctuating velocities of small particles suspended in a fluid stream are determined. The seeding of small particles is necessary to provide scattered light for the Laser-Doppler instrument. The question then arises: "How well do the particles follow the flow?" This report considers the motion of a single particle or group of particles in a fluid stream with emphasis on solid particles in a gas. Flow in pipes and in an isothermal round free jet are used as examples.

Motion of a single particle is a simplified case of dilute gas-solid suspension flow. Large particles will only follow the slow large scale turbulent motions of fluid, while particles small compared to the smallest scale of turbulence will respond to all turbulence components of the fluid. Since the particle contributes to energy dissipation due to lags between particle and fluid, large numbers of particles will modify the energy spectrum of the fluid.

Many studies on particle fluid interactions have been made because this problem is of importance in several fields. The motions of small particles have been analyzed by comparisons of the amplitudes of oscillations of particle and fluid in an accoustic field, and by comparison of the mean velocities in turbulent flow. Special problems exist when solid boundaries are present or particle-particle interactions are important. At speeds below the velocity of sound the difference velocity between fluid and solid is near the continuum regime and viscous effects are important. Corrections for compressibility and rarefaction are necessary for higher speeds when slip or transition flows are encountered.

The results of calculations on particle fluid interactions for small particles generally show that individual particles below one micron in diameter follow the flow. Turbulence measurements on particles are then a good representation of the fluid behavior as long as the turbulent fluctuations are not extremely rapid. Further work is necessary to consider the energy dissipation range of some turbulent flows or high speed flows.

In the following pages the velocity of the fluid and particle are compared for several conditions of physical interest. First the mean velocity and then the velocity fluctuations are calculated for a single particle. A survey of the literature on experimental work is also presented. Finally some consideration of multiparticle systems is given. Although the equations are the same, the conclusions for flow in a liquid are much different from those given in this report for a gase.

Extensive introductions to the field are available in the books by Fuchs [1] and Soo [2]. These references have been used extensively in this report.

I. ONE DIMENSIONAL MEAN VELOCITY OF SINGLE PARTICLES

We begin with the simplified case of one dimensional flow when the particle does not distrub the fluid motion.

The equation of motion for a single spherical particle in creeping flow is given in many texts as:

$$m \frac{dV}{dt} = 6\pi\mu r\ (U-V) - \frac{m'}{\rho}\frac{dp}{dz} - \frac{m'}{2}\left(\frac{dV}{dt} - \frac{dU}{dt}\right) - 6r^2\sqrt{\pi\mu\rho}\int_{t_o}^{t}\frac{d(V-U)}{d\tau}\frac{d\tau}{\sqrt{t-\tau}} + F_e \tag{1.1}$$

This equation was originally obtained by Basset [3] and is discussed by Tchen [4] and Hinze [5]. The notation is as follows:

m = mass of particle = $\frac{4}{3}\pi r^3\rho_p$

m' = mass of fluid = $\frac{4}{3}\pi r^3\rho$

V = particle velocity

U = fluid velocity

μ = fluid viscosity

ρ = fluid density

ρ_p = particle density

r = particle radius

t = time

F_e = external potential force

Equation 1.1 then equates the force to accelerate a particle to the following in order of their appearance in the equation:

1. Viscous drag on the particle for slow relative motion.

2. Pressure gradient in the fluid surrounding the particle.
3. Force to accelerate the apparent mass of the particle relative to the fluid.
4. The effect of acceleration on the viscous drag. (Basset force)
5. The external potential force such as gravity.

To account for instantaneous motion in a turbulent field, this equation must be written in vector form in the proper frame of reference. However, the equation as it stands can be used to determine the behavior of the mean flow. In a later section the particle velocity in a fluctuating medium will be considered. In general the pressure term can be obtained from the equation of motion of the fluid assuming the particles do not have an effect on the fluid behavior. The equation then depends upon the viscous forces and inertial forces in the fluid and the results will be functions of velocity gradient (dv/dz) and the gradient of velocity gradient (d^2v/dz^2). In this discussion these terms are assumed small or that any effect can be included in an experimental drag coefficient.

That is the viscous drag term in Equation 1.1 is replaced by $mF_D(U-V)$ where

$$F = \frac{3}{8} C_D \frac{\rho}{\rho_p r} (U-V)$$

and C_D is the drag coefficient. At low particle Reynolds number, $\frac{2r(U-V)\rho}{\mu}$, the first term in Equation 1.1 is obtained.

If the particle is in a fluid moving with constant velocity, the Basset force is neglected and the pressure gradient and external potential force are constant, the solution to Equation 1.1 is:

$$U-V = \frac{2r^2\left(-\frac{dp}{dz} + \frac{3F_e}{4\pi r^3}\right)}{9\mu}\left[1 - e^{-\frac{9\mu t}{r^2(2\rho_p+\rho)}}\right], \qquad (1.2)$$

when at t = 0, the particle and fluid have the same velocities. The largest difference then occurs at $t = \infty$ and the factor $\frac{2r^2}{9\mu}\left(-\frac{dp}{dz}\right)$ need only be considered in the absence of a potential force. For flow in a pipe the pressure drop is a function of the pipe diameter, D, and average velocity, $\langle v\rangle$. In terms of the Fanning friction factor, f,

$$-\frac{dp}{dz} = \frac{2f}{D}\rho\langle v\rangle^2.$$

The friction factor is given by:

$$f = 0.0791\ N_{Re}^{1/4}$$

at Reynolds numbers between 10^4 and 10^5 but for purposes of comparison it can be assumed that the result holds for higher fluid Reynolds numbers. Then:

$$\frac{(U-V)_\infty}{\langle V\rangle} = .0088\left(\frac{r}{R}\right)^2 N_{Re}^{3/4} \qquad (1.3)$$

where R is the pipe radius. To obtain less than 1% relative error at $N_{Re} = 10^6$ in a 4 inch diameter pipe a particle less than 300 microns in radius is required. If the pipe is vertical, the potential force due to gravity must be included.

$$\frac{3}{4\pi r^3}F_e = (\rho_p - \rho)\ g$$

Then:

$$\frac{(U-V)_\infty}{\langle v \rangle} = .0088\ \left(\frac{r}{R}\right)^2 N_{Re}^{3/4} + \frac{2}{9\mu}\frac{r^2 g(\rho_p - \rho)}{\langle v \rangle}$$

$$\sim \frac{2r^2 g\rho_p}{9\mu\langle v \rangle}$$

When $\rho_p = 1.0$ g/cm^3 and $\mu = 2 \times 10^{-4}$ g/cm sec.,

$$\frac{(U-V)_\infty}{\langle v \rangle} \sim \frac{10^6 r^2}{\langle v \rangle}$$

The gravity force is larger than the pressure force and results in a lower particle size limit for a 1% error. This limit is approximately equal to $\langle v \rangle^{1/2}$ microns when the velocity is given in cm./sec. For example under the same conditions as above a 95μ diameter particle is the 1% limit while a 300 micron particle would give an error over 10% when the fluid stream is air and the particle density is 1.0 g/cm^3.

The analysis appears valid for pipe flow mean velocities in isothermal turbulent flow when compared with experimental data. Recently Reddy, Wijk and Pei measured particle and fluid velocities in a 10 cm. diameter vertical pipe [6]. Using 200 micron particles the error at the centerline was 16%. Assuming they used alumina particles with a density of 2.42 g/cm^3 the calculated error at t = ∞ is 25%. The agreement is good and could be improved by using a correction to the viscous drag.

If the terminal velocity is not reached, the particles may show variations in velocity due to different times of approach to terminal conditions.

It is important to keep the velocity error less than 1% if this is to be avoided.

Hughes and Gilliland [7] showed the results of Basset's solution to Equation 1.1 for motion of a particle in a fluid at rest. The terminal velocity is not changed by the addition of the integral term (Basset force) when the pressure gradient and external forces are constant and the fluid velocity is also constant. This can be easily shown by the Fourier transform method which is explained in Chapter II of this report. The transient curves, however, are changed. The plot given by Hughes and Gilliland shows little difference in the transient curves when $\rho_p/\rho \sim 10^3$ but for $\rho_p/\rho < 10$ the corrections are significant.

The next problem to be considered is to add acceleration of the fluid as would be encountered in the free jet. Again the Basset term will be neglected. Also the external force will be dropped and the assumption made that:

$$- \frac{dp}{dz} = \rho \frac{dU}{dt}$$

from the Navier-Stokes equation of fluid motion. Then:

$$\frac{2}{3} r^3(2\rho_p + \rho) \left(\frac{dV}{dt} - \frac{dU}{dt}\right) + 6\mu r \, (V-U) = - \frac{4}{3} r^3(\rho_p - \rho) \frac{dU}{dt} \qquad (1.4)$$

If the velocity varies linearly with downstream distance, Z,

$$U = U_o + \delta z, \qquad (1.5)$$

where δ is a constant.

Since

$$U = dz/dt$$

$$\frac{dU}{dt} = \delta U \tag{1.6}$$

And

$$U = U_\circ e^{\delta t} \tag{1.7}$$

Solving Equation 1.4 then gives

$$\frac{U-V}{U} = \frac{2\delta(\rho_p - \rho)}{(2\rho_p + \rho)(\varepsilon + \delta)}\left[1 - e^{-(\delta+\varepsilon)t}\right] \tag{1.8}$$

Where

$$\varepsilon = \frac{9\mu}{r^2(2\rho_p + \rho)}.$$

At the centerline of a round free jet the mean velocity decreases almost linearly for the first 21 diameters after the velocity decrease begins as shown by Corrsin [8]. In this region the parameter δ becomes approximately

$$\delta = -\,0.05\,\frac{U_\circ}{d}\ ,$$

where $U_\circ$ is the velocity at the jet exit and d the jet diameter. Errors are less than 1% for particles less than 10 microns when the particle density is one gram per cm^3 for $\delta = 10$. Similar calculations have been made by Gilbert, Davis and Altman [9] for the transient case. In supersonic flow $\delta > 500$ and particles less than one micron radius are necessary to have less than 1% error considering an infinite time.

Inclusion of the Basset force will effect the transient behavior but not significantly the terminal velocity difference at infinite time. Measurements of particle mean velocities will, therefore, closely approximate the mean stream velocity when the particle size is on the order of one micron.

A general solution to equation 1.4 including the gravity term was given by Tchen but the solution is difficult to apply. Most measurements are taken under conditions where the time from the flow source is much shorter than that to reach the terminal velocity. Therefore, errors in mean velocities are less than the figures used in the illustrations above.

Deviations from the creeping flow assumption occur when the particle Reynolds number is greater than 0.1. Empirical equations can be used to modify a drag coefficient in Equation 1.1 for these higher Reynolds numbers. The results will lead to a reduction in velocity lag and are discussed in the section on turbulent flow. Numberous theoretical studies are available in the literature on the flow of a compressible gas containing solid particles. A review up to 1966 has been given by James, Babcock and Seifert [10]. In this report the effects of compressibility and rarefaction will only be considered in the section on turbulent fluctuations.

Only a limited number of experimental studies have been made in which the particle and fluid velocities are measured. These are listed below with a short description of the results.

1. Recent Studies of Mean Velocities in Pipes

   1969 - Reddy, Van Wijk and Pei [6] - Measured air and particle velocities in 10 cm. tube at Air Reynolds number of 55,000. At centerline 200μ particle velocity was 8.13 m/sec compared to 9.8 m/sec for the air.

1968 - McCarthy and Olsen [11] - Summarizes work on drag coefficients and measures particle and fluid velocity in a pipe for 64 micron glass beads and 3 micron $CaCO_3$ in accelerating flow. After the initial entry the velocity of the 3μ particles was indistinguishable from the gas while the 64μ particles had a velocity 10% less than the air velocity. Using the formula

$$\frac{dV}{dz} = \frac{3C_D\rho(U-V)^2}{8\rho_p rV}$$

They found good agreement with the experiment when C_D was the standard drag coefficient. Their results support the work of Torobin and Gauven [12] who found that wake interaction and free stream turbulence can be neglected in dilute particle suspensions.

2. Recent Studies of Mean Velocities in Nozzles or Jets.

1969 - Morse, Tullis, Seifert and Babcock [13] - Used a laser Doppler method for nozzle flows. In their Al_2O_3 system errors of 6.8% for a one micron particle to 41.9% for a 7 micron particle were predicted. From the particle size distribution they matched the signal amplitude vs velocity. However, signals at lower velocities were unexplained by a collisionless model. Computations based on the effect of collisions showed that smaller particles would undergo large velocity changes in collisions with larger ones. They concluded that particle size distribution must be known in order to calculate the velocity distribution and particle collisions must be included in the model for calculating velocity lags.

1968 - James, Babcock and Seifert [14] - Used a laser-Doppler technique to measure nozzle flows. Indicated that particle collisions are important at low velocities. Results agreed with calculated according to the authors but no quantative values are given.

1965 - Fulmer and Wirtz [15] - Measured photographically the particle and gas flow at a nozzle exit as a function of particle size. The gas velocity was 2,900 feet per second. Figure 1.1 is a plot of the data for the aluminum powder velocity - gas velocity ratio vs the particle diameter.

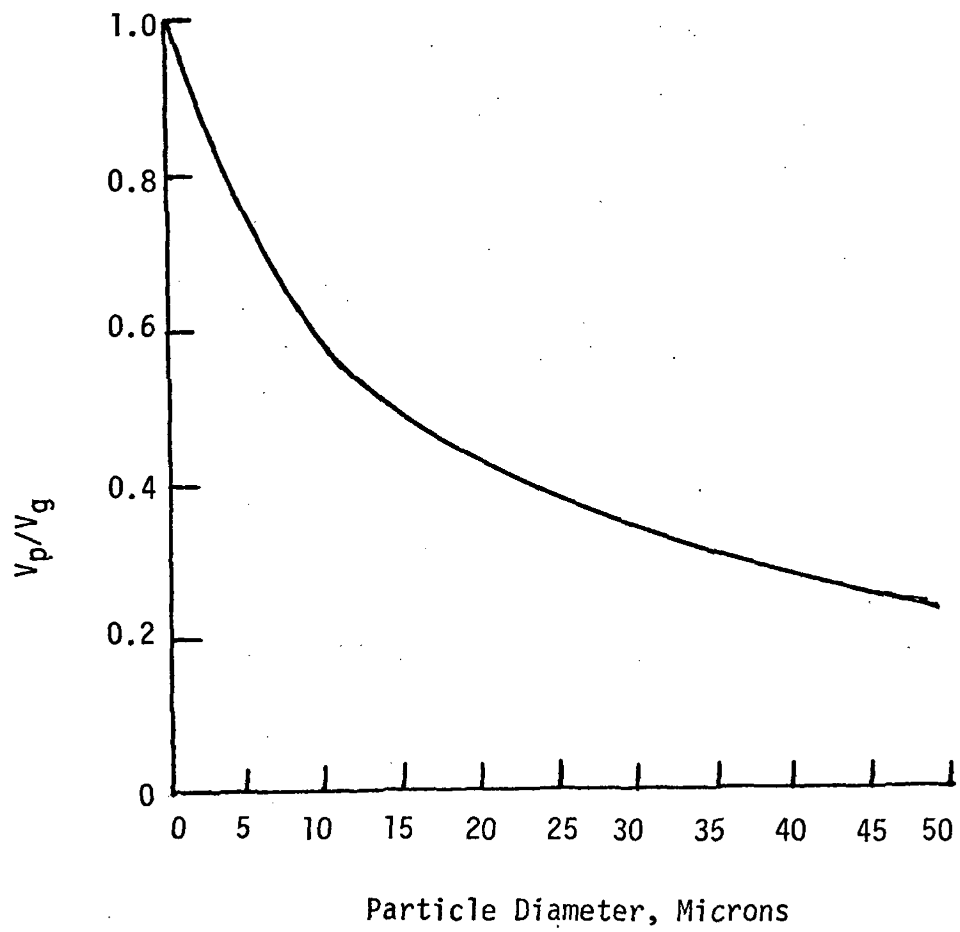

Figure 1.1 Mean Velocity Lags in Nozzle Flow. Gas Velocity 2900 ft/sec. From Fulmer and Wirtz [15].

Other references are listed by Soo [2] for the pipe flow case but no others could be found for the nozzle flow. Measurements on turbulent spectra and fluctuations will be discussed in a later section.

Another factor often questioned is the effect of particle rotation. Afanasev and Nikolaevskii [16] have shown that the rotational oscillations of a solid particle decay exponentially with characteristic relaxation time

$$\tau_\omega = \frac{1}{15}\frac{r^2}{\mu}\rho_p$$

Small particles in air then will equilibrate very rapidly to the condition of the surrounding fluid. A one micron particle with density of 1 g/cm^3 has a decay proportional to exp(- 3 x 10^5t) when t is in seconds. Only particles over 100 microns in radius would maintain their rotation for a sufficient time to effect results unless very short times are investigated. In mean velocity measurements, rotation is not significant; but for turbulent fluctuation measurements these decay times may be significant in small eddies.

Rotation of a solid particle in a fluid stream can be created in many ways including:

1. Velocity gradients in the flow field.
2. Collisions with solid boundaries.
3. Collisions with other particles.

A rotating particle adds a lift force to the equation of motion but does not effect the drag coefficient unless the relative Reynolds number is high. At the high Reynolds numbers rotation thickens the boundary layer and changes the characteristics of flow separation.[17]

Some studies of the effects of rotation have been made by Rubinow and Keller [18], Eichhorn and Small [19] and Saffman [20]. Although Saffman concludes the result of Rubinow and Keller is high, their lift force is to the first order

$$F_L = \pi r^3 \rho \vec{\Omega} \times \vec{V}$$

where $\vec{\Omega}$ is the vector angular velocity. For small spheres on the order of one micron in diameter in air, the angular velocity must be very large before this term is significant.

The ratio of the magnitude of lift force to drag force is approximately [2]

$$\frac{|F_L|}{|F_D|} = \frac{1}{6} \frac{r^2 \omega \rho}{\mu} \quad .$$

For a one micron particle in air at a rotational frequency of 20 KHz this amounts to only 6%, but for particles two microns or larger this force is significant at high frequencies. Another discussion of the left problem has been recently given by Kondic [21].

II. MOTION OF PARTICLES IN AN OSCILLATING FLUID

Although turbulence is composed of random fluctuations, before an attempt is made to consider turbulent fluctuations, it is well to examine fluctuations of a single frequency. The one dimensional equation of motion of a particle in a vibrating medium consists of Equation 1.1 plus terms due to the oscillation. Additional terms, one proportional to the velocity which increases the drag and one proportional to the acceleration which increases the inertia part are required. The extra forces added to Equation 1.1 are:

$$F_{osc} = -\frac{9}{4} m'\omega_o\beta\ (V-U) - \frac{9}{4} m'\beta \left(\frac{dV}{dt} - \frac{dU}{dt}\right) \tag{2.1}$$

Where ω_o is the frequency in sec.$^{-1}$ and $\beta = \frac{1}{r}\sqrt{2\mu/\rho\omega_o}$. This formula is derived in Lamb [22], and Landau and Lifshitz [23] based on the earlier work of Stokes. The equation of motion is then:

$$m\frac{dV}{dt} = m'\frac{dU}{dt} - \frac{9}{4} m'\ \omega_o\beta(1 + \beta)(V-U)$$
$$- m'\left(\frac{1}{2} + \frac{9}{4}\beta\right)\left(\frac{dV}{dt} - \frac{dU}{dt}\right) - 6r^2\sqrt{\pi\mu\rho}\int_{t_o}^{t}\frac{d(V-U)}{d\tau}\frac{d\tau}{\sqrt{t-\tau}} \tag{2.2}$$

or in terms of $\Delta = U-V$

$$\left[m + m'\left(\frac{1}{2} + \frac{9}{4}\beta\right)\right]\frac{d\Delta}{dt} + \frac{9}{4} m'\omega_o\beta(1 + \beta)\Delta + 6r^2\sqrt{\pi\mu\rho}\int_{t_o}^{t}\frac{d\Delta}{d\tau}\frac{d\tau}{\sqrt{t-\tau}} = (m-m')\frac{dU}{dt} \tag{2.3}$$

This equation is easily solved using a Fourier integral transform:

$$F(\omega) = \int_{-\infty}^{\infty} e^{-i\omega t} f(t)dt \tag{2.4}$$

and the inverse transform

$$f(t) = \frac{1}{2\pi} \int_{-\infty}^{\infty} e^{i\omega t} F(\omega)d\omega \tag{2.5}$$

We assume $U = U_0 \sin \omega_0 t$ and t_0, the starting time is minus infinity. Then the integral term has a simple transform and the transform of the $\sin \omega_0 t$ and $\cos \omega_0 t$ are Dirac delta functions. The inverse transform needs no integration. $F(\omega)$ is evaluated at two points to give $f(t)$, or the amplitude of the response can be obtained directly from the square root of the product of the transform with its complex conjugate.

Let us write Equation2.3 as:

$$\varepsilon \frac{d\Delta}{dt} + \xi\Delta + \gamma \int_{-\infty}^{t} \frac{d\Delta}{d\tau} \frac{d\tau}{\sqrt{t-\tau}} = U_0\omega_0(m - m') \cos \omega_0 t \tag{2.6}$$

If $\Delta = 0$ at the starting time $(-\infty)$, the transform, $\tilde{\Delta}(\omega)$ is

$$\tilde{\Delta}(\omega) = \frac{U_0\omega_0(m - m')\pi[\delta(\omega - \omega_0) + \delta(\omega + \omega_0)]}{i\omega\varepsilon + \xi + \gamma(1 + i)\omega^{\frac{1}{2}} \sqrt{\pi/2}} \tag{2.7}$$

Then the inverse after some manipulation becomes

$$\frac{\Delta(t)}{U_0} = \frac{\omega_0(m - m')}{(\xi + \delta\omega_0^{\frac{1}{2}} \sqrt{\pi/2})^2 + (\omega\varepsilon + \delta\omega_0^{\frac{1}{2}} \sqrt{\pi/2})^2} \times$$

$$\left\{\left(\xi + \delta\omega_o^{\frac{1}{2}} \sqrt{\pi/2}\right) \cos \omega_o t + \left(\omega\varepsilon + \delta\omega_o^{\frac{1}{2}} \sqrt{\pi/2}\right) \sin \omega_o t\right\} \tag{2.8}$$

Or:

$$\frac{\Delta(t)}{U_o} = \frac{\omega_o(m - m')}{\left[(\xi + \delta\omega_o^{\frac{1}{2}} \sqrt{\pi/2})^2 + (\omega\varepsilon + \delta\omega_o^{\frac{1}{2}} \sqrt{\pi/2})^2\right]^{\frac{1}{2}}} \sin (\omega_o t + \phi) \tag{2.9}$$

Where:

$$\tan \phi = \frac{\xi + \delta\omega_o^{\frac{1}{2}} \sqrt{\pi/2}}{\omega\varepsilon + \delta\omega_o^{\frac{1}{2}} \sqrt{\pi/2}} \tag{2.10}$$

In terms of r, ρ, ρ_p and μ the amplitude is then:

$$\text{Amp.} \frac{\Delta(t)}{U_o} = \frac{\Delta_o}{U_o} = \frac{\left(\frac{\rho_p}{\rho} - 1\right)}{\left\{\left[\frac{9}{4} \beta(1 + \beta) + \frac{9}{4\sqrt{2}} \beta\right]^2 + \left[\frac{\rho_p}{\rho} + \frac{1}{2} + \frac{9}{4} \beta + \frac{9}{4\sqrt{2}} \beta\right]^2\right\}^{\frac{1}{2}}} \tag{2.11}$$

which is a function of ρ_p/ρ and β only. This particular form of the comparision is not found in the literature and it is convenient to solve Equation 2.8 for V(t) to compare amplitudes directly. The result is

$$\frac{V}{U_o} = V_o \sin (\omega t - \psi) \tag{2.12}$$

Where

$$V_o = \left[1 + \Delta_o^2 \left(1 - \frac{2(\frac{\rho_p}{\rho} + \frac{1}{2} + \frac{9}{4} \beta + \frac{9}{4\sqrt{2}} \beta)}{\left(\frac{\rho_p}{\rho} - 1\right)}\right)\right]^{\frac{1}{2}} \tag{2.13}$$

and

$$\tan \psi = \frac{\left(\xi + \delta\omega_o^{\frac{1}{2}} \sqrt{\pi/2}\right) \omega_o(m-m')}{\left(\xi + \delta\omega_o^{\frac{1}{2}} \sqrt{\pi/2}\right)^2 + \left(\omega\varepsilon + \delta\omega_o^{\frac{1}{2}} \sqrt{\pi/2}\right)^2 - \omega_o(m-m')\left(\omega\varepsilon+\delta\omega_o^{\frac{1}{2}}\sqrt{\pi/2}\right)} \tag{2.14}$$

NEW ADDRESSES TO BE ADDED TO THE WESTERN STATES SECTION

THE COMBUSTION INSTITUTE

Mr. Earl C. Miller
7 Terrace Drive
Worcester, Mass. 01609

Jet Propulsion Laboratory
Attn: Library, Reference 111-113
4800 Oak Grove Drive
Pasdena, California 91103

Tim T. Fu
1384 Isla Court
Camarillo, California 93010

To compare with previous results we consider simplifications of Equation 2.2 and their solutions.

If all the terms on the right hand side of Equation 2.2 are discarded except $\frac{9}{4} m'\omega\beta^2(V-U)$, the resulting equation represents motion in a medium whose resistance is non-inertial. Then for $U = U_o \sin \omega t$,

$$m \frac{dV}{dt} + \frac{9}{4} m' \omega\beta^2 V = \frac{9}{4} m' \omega\beta^2 U_o \sin \omega t \tag{2.15}$$

The amplitude of the solution is

$$\frac{V_o}{U_o} = \frac{1}{\sqrt{1 + \left(\frac{2r^2 \rho_p \omega}{9\mu}\right)^2}} \tag{2.16}$$

Equation 2.16 was used by Rosenweig, Hottle and Williams [24] to justify their light scattering measurements of smoke to determine turbulence fluctuations. Fuchs [1] cites several experimental confirmations of this expression and also shows that the solution to Equation 2.2 without the integral term gives almost identical results. Since the experimental data scatter widely, there is some doubt of the validity of the analysis.

The solution to eq. 2.2 without the integral term has been widely used since its derivation by Konig [25]. The result is

$$\frac{V_o}{U_o} = \left[\frac{1 + 3\beta + 9\beta^2 + \frac{9}{}\beta^3 + \frac{9}{4}\beta^4}{g^2 + 3g\beta + \frac{9}{2}\beta^2 + \frac{9}{2}\beta^3 + \frac{9}{4}\beta^4}\right]^{\frac{1}{2}} \tag{2.17}$$

where $g = \frac{1}{3}(2\frac{\rho_p}{\rho} + 1)$. Since in all cases the amplitudes are functions of $r\sqrt{\omega}$ and ρ_p/ρ, plots can be made by varying these two parameters. Figures 2.1 and 2.2 show such plots.

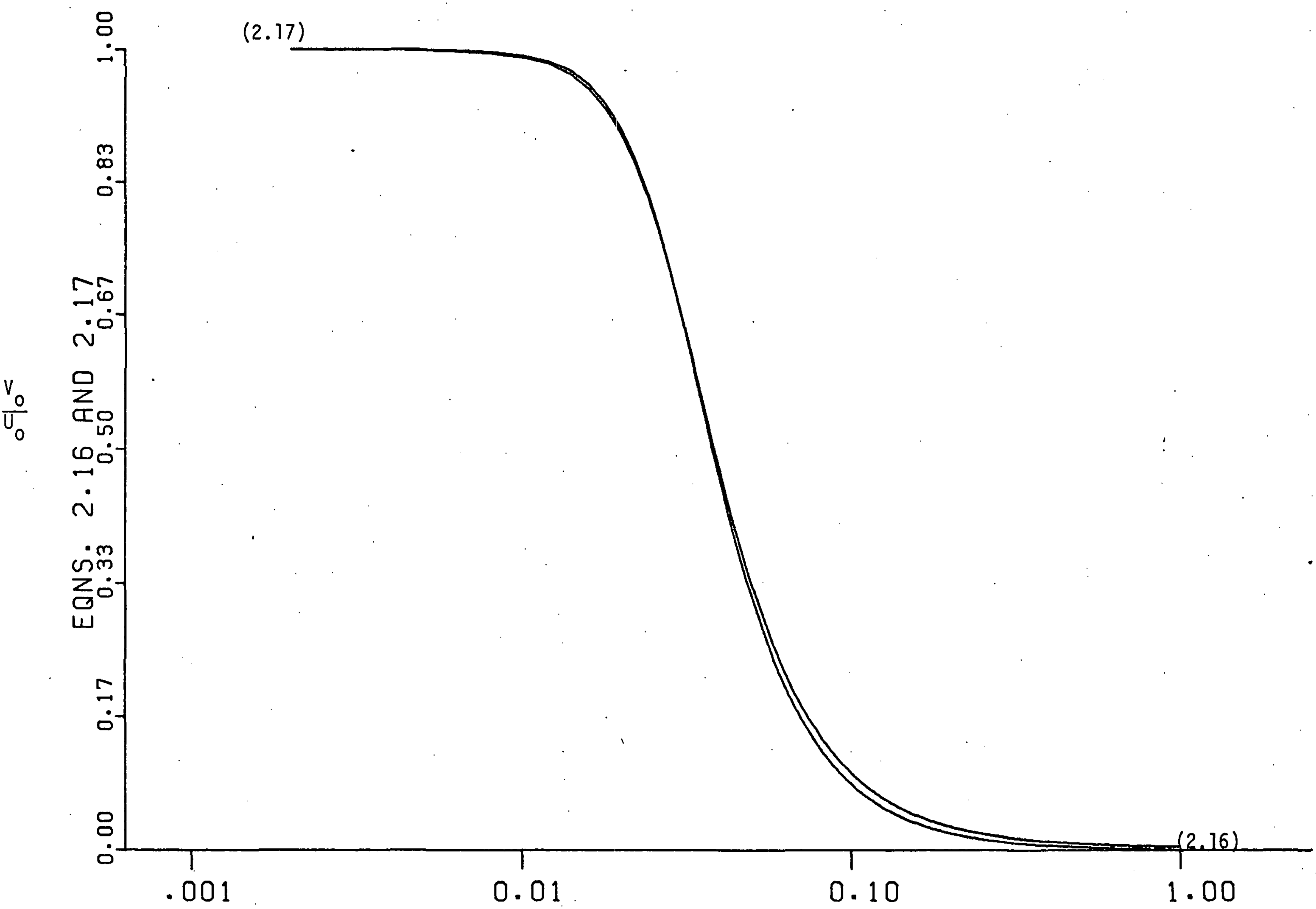

(2.17)
(2.16)
1.00
0.83
0.67
0.50
0.33
0.17
0.00
EQNS. 2.16 AND 2.17
$\frac{V_o}{U_o}$
.001
0.01
0.10
1.00
R*SQRT(OMEGA)

FIGURE 2.1

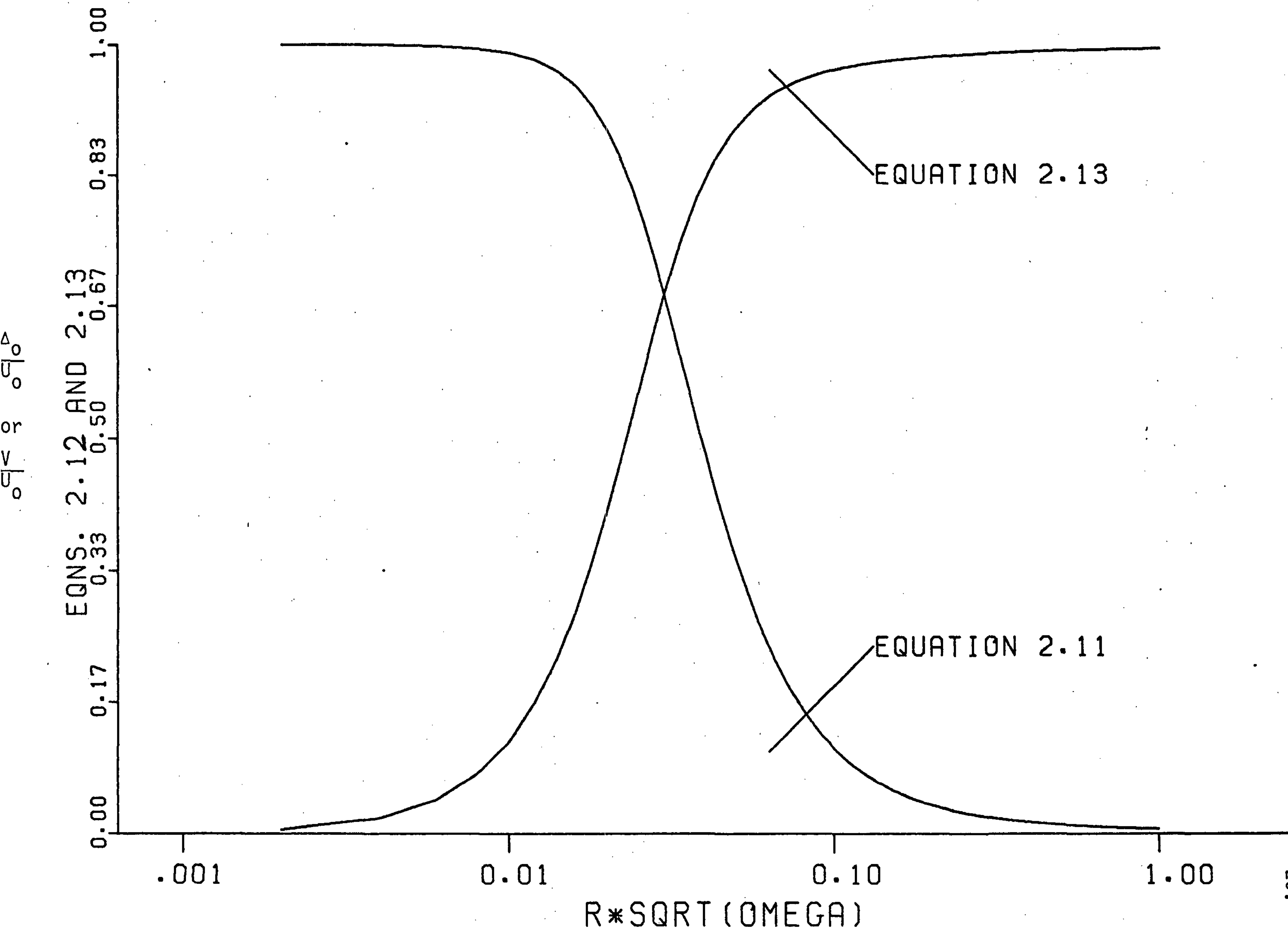
1.00
0.83
0.67
0.50
0.33
0.17
0.00
EQNS. 2.12 AND 2.13
or
EQUATION 2.13
EQUATION 2.11
.001
0.01
0.10
1.00
R*SQRT(OMEGA)

FIGURE 2.2

In the first, Figure 2.1, Equations 2.16 and 2.17 are plotted for air at room temperature and for a particle density of $1.0 g/cm^3$. Figure 2.2 shows equations 2.12 and 2.13 for the same conditions. Equation 2.16 would apply only for low relative Reynolds numbers between particle and fluid and in the absence of other forces. Fuchs lists additional forces such as hydrodynamic sound pressure due to changes in density of the gas which cause particles in a standing wave to drive to the nodes. Other effects are scattering and absorption of sound waves, hydrodynamic interaction between particles and electrostatic scattering of particles. Little is known about the importance of these forces as functions of concentration, mean velocity or frequency.

III. MOTION OF A SINGLE PARTICLE IN A TURBULENT FLUID

In turbulent flow the oscillations do not occur at one frequency or amplitude but vary in time and space. Although the acoustic wave gives apparent agreement with single frequency experiments, it would not account for the frequency spectrum found in turbulence. If the measuring instrument is able to determine precisely the instantaneous velocities, the only errors in using the results for the fluid velocity will be the difference between the fluid and particle. Most instruments measure the velocities over a finite volume and a finite time span. Therefore a distribution of velocities is obtained. The problem of investigating the relationship between the measured distribution and the true distribution involves the simultaneous consideration of the instrument, the particle lags and the fluctuations due to turbulence. Only the interaction between the particle lag and the turbulent fluctuations are considered in this report. A possible way to allow for turbulence is to assume that Equation 2.17 also applies to the ratio of amplitudes of the frequency spectra curves of particle and fluid turbulence.

Then

$$\left(\frac{V_0^2}{U_0^2}\right)^{\frac{1}{2}} = \int_0^{\infty} F(\omega)\,\frac{V_0(\omega)}{V_0}\,d\omega$$

where $F(\omega)$ is the amplitude of the normalized frequency spectra density curves for the fluid and $\overline{V^2}$, and $\overline{U^2}$ are time mean square averages. A similar expression can be obtained for the relative velocity $V_r = V\text{-}U$. We will compare Equation 3.1 with another analysis for examples of $F(\omega)$ obtained from experiments later.

As in the case of the acoustic field the equation of motion of a particle in a turbulent field is obtained from the momentum balance.

$$m \frac{dV}{dt} = \sum \quad \text{Forces},$$

where

$$\frac{dV}{dt} = \frac{\partial \vec{V}}{\partial t} + (\vec{V}.\nabla)\vec{V}$$

in vector notation. For simplicity the vector symbol will be dropped. For a spherical particle when continuum equations are valid the forces are the following:

1) Gravity = mg
2) Buoyancy = m'g
3) The variation of hydrostatic pressure in the fluid = $m' \dfrac{dU}{dt'}$, where the substantial derivative is based on the fluid velocity (indicated by $\dfrac{d}{dt'} = \dfrac{\partial}{\partial t} + U.\nabla$)
4) The force necessary to accelerate the "apparent" mass of the particle relative to ambient flow = $\frac{1}{2} m' \left[\dfrac{dU}{dt} - \dfrac{dV}{dt}\right]$.
5) The deviation of the flow pattern from steady state (Basset force) =

$$6r^2 \sqrt{\pi\rho\mu} \int_{t_0}^{t} \frac{\frac{dU}{d\tau} - \frac{dV}{d\tau}}{\sqrt{t-\tau}}$$

6) The drag force = $mF_D(U-V)$

7) The Lift due to spin.

8) The pressure = $\frac{4}{3}\pi r^3 \nabla p$

9) Intermolecular forces.

10) Forces induced in the neighborhood of an interface.

11) Forces due to temperature gradients in fluid or particle.

12) Forces due to molecular diffusion.

13) The force due to oscillating pressure

14) Other body forces

Only 3, 4, 5, 6, and 8 are usually retained in the equation of motion.

These terms form an equation which has been solved only when additional assumptions are valid. Here we take a modification of the approach given by Soo [2] based on solutions by Tchen and Chao. The assumptions are

a) The particle is small and spherical so that a simple expression can be used for the drag coefficient based on the relative motion. The drag coefficient appears in 6) above when $F_D = \frac{3}{8} C_D \frac{\rho}{\rho_p r} |U-V|$.

Torobin and Gauvin [26] have reviewed the effect of turbulence on C_D. Literature results show both increased and decreased drag coefficients. An empirical correction which fits the standard drag curve over a large range of particle Reynolds numbers is given by Torobin and Gauvin and is convenient for computer calculations.

$$C_o = \frac{24}{N_{Re}} (1 + 0.15\, N_{Re}^{0.687}) \tag{3.2}$$

where $N_{Re} = \frac{2r(U-V)\rho}{\mu}$.

At high speeds approaching sonic velocity the drag coefficient can be modified to include effects of gas compressibility and rarefaction [27]. If the effects of velocity gradient and derivatives of velocity gradient can be expressed as a constant multiplied by the relative velocity, the drag coefficient can be further modified.

Let $$K = \frac{C_D \text{ (modified)}}{C_D \text{ (Stokes)}} , \tag{3.3}$$

Then only the factor K will appear in the equation of motion. K is a function of the variables mentioned above.

b) The particle is small compared to the smallest wavelength of turbulence.

c) The flow field is not perturbed by the presence of the solid particle. Then the components of the pressure term can be taken from the Navier - Stokes equation for the single phase fluid.

$$-\nabla p = \rho\frac{DU}{Dt} - \mu\nabla^2 U,$$

where

$$\frac{DU}{Dt} = \frac{\partial U}{\partial t} + U\cdot\nabla U.$$

When a cloud of particles is present this equation includes the effects of flow around the solid. A modification of this can be made if we can include the effect of the nonlinear terms in the drag coefficient.

d) The path of the solid particle coincides with the fluid streamline. That is $\frac{d}{dt} = \frac{d}{dt^{\tau}}$.

This assumption leads to the conclusion that the particle diffusivity is the same as the Lagrangion eddy diffusivity of turbulence. Soo discusses the experimental and theoretical reasons why this is not true for a finite size particle. The particle diffusivity is a function of particle response time and the Lagrangion and Eulerian scales of turbulence. However, without the assumption that the particle and fluid paths coincide, no rigorous solution to the equation of motion is available [28].

e) The turbulence is homogeneous and steady. Then a simple velocity spectrum can be used. Also the mean flow can be omitted from the equations by having the coordinates follow the mean motion. This assumption has been discussed in Section I. If we use a coordinate system which moves with the particle, the total time derivatives of the fluid velocity must be replaced by the derivative moving with the coordinate system:

$$\frac{dU}{dt^{\tau}} = \frac{\partial U}{\partial t} + (V\cdot\nabla)U \tag{3.4}$$

f) The turbulence is not effected by solid boundaries and the starting time, t_0, in the Basset force term can be set at minus infinity.

With these assumptions the equation of motion becomes

$$m \frac{dV}{dt} = 6\pi\mu rK(U-V) + m' \left[\frac{\partial u}{\partial t} + (U\cdot\nabla)\, U - \nu\nabla^2 U\right]$$

$$+ \frac{1}{2}m' \left[\frac{dU}{dt} - \frac{dV}{dt}\right] + 6r^2\sqrt{\pi\rho\mu}\int_{-\infty}^{t} \frac{d(U-V)}{dt} \frac{d\tau}{\sqrt{t-\tau}} \qquad (3.5)$$

Or

$$\frac{dV}{dt} = \frac{-2\nabla p}{2\rho_p+\rho} + \frac{9\mu K}{r^2\left(2\rho_p+\rho\right)}(U-V) + \frac{\rho}{2\rho_p+\rho}\frac{dU}{dt}$$

$$+ \frac{9}{\left(2\rho_p+\rho\right) r}\sqrt{\frac{\rho\mu}{\pi}}\int_{-\infty}^{t} \frac{\frac{d}{d\tau}(U-V)}{\sqrt{t-\tau}}\, d\tau \qquad (3.6)$$

Now let $\alpha = \frac{3\mu}{\rho r^2}$, and $\delta = \frac{3\rho}{2\rho_p+\rho}$, then:

$$\frac{dV}{dt} = -\frac{2\delta}{3\rho}\nabla p + \alpha\delta K(U-V) + \frac{1}{3}\delta\frac{dU}{dt} + \delta\sqrt{\frac{3\alpha}{\pi}}\int_{-\infty}^{t} \frac{\frac{d}{d\tau}(U-V)}{\sqrt{t-\tau}}\, d\tau \qquad (3.6a)$$

To write the components of equation 3.6 in a cartesian coordinate system we have

$$\frac{dV_i}{dt} = \frac{\partial V_i}{\partial t} + (V\cdot\nabla)\, V_i = \left(\frac{dV}{dt}\right)_i \qquad (3.7)$$

and we note that

$$\frac{\partial u}{\partial t} + (U\cdot\nabla)U = \frac{\partial U}{\partial t} + (V\cdot\nabla)U + [(U-V)\cdot\nabla]U = \frac{dU}{dt} + [(U-V)\cdot\nabla]U. \qquad (3.8)$$

So that

$$\left[\frac{\partial U}{\partial t} + (U\cdot\nabla)U\right]_i = \frac{dU_i}{dt} + (U_i - V_i)\,\frac{\partial U_i}{\partial X_i} + (U_j - V_j)\,\frac{\partial U_i}{\partial X_j} + (U_k - V_k)\,\frac{\partial U_i}{\partial X_k}$$

Then equation 3.6a becomes

$$\frac{dV_i}{dt} = \delta\,\frac{dU_i}{dt} + \alpha\delta K\,(U_i - V_i) + \frac{2}{3}\,\delta(U_i - V_i)\frac{\partial U_i}{\partial X_i} + \frac{2}{3}\,\delta(U_j - V_j)\,\frac{\partial U_i}{\partial X_j}$$

$$+ \frac{2}{3}\,\delta\,(U_k - V_k)\,\frac{\partial U_i}{\partial X_k} - \frac{2}{3}\,\nu\delta\nabla^2 U_i + \delta\left(\frac{3\alpha}{\pi}\right)^{\frac{1}{2}}\int_{-\infty}^{t}\frac{\frac{d}{d\tau}\,(U_i - V_i)\,d\tau}{\sqrt{t-\tau}} \qquad (3.9)$$

This derivation is also given by Hinze [5], and it represents the particle motion from a Lagranian point of view. That is the particle follows the detailed motion of the fluid. Friedlander [29] suggested a Eulerian formulation when the particle is large. The true situation lies in between the Lograngian and Eulerian models. A short discussion of this point and a review of the literature pointing out the important parts of the preceeding derivation is given by Brodkey [30].

Equation 3.9 contains three nonlinear terms and the term involving the second derivative with respect to the space coordinates. Conditions for the neglect of these terms have been given by Corrsin and Lumley [31] and Hinze [5]. A similar argument is given here. Let us assume that (U_j-V_j) and (U_k-V_k) are porportional to (U_i-V_i). Then the nonlinear terms can be grouped together

$$\frac{2}{3}\,\delta(U_i-V_i)\left[\frac{\partial U_i}{\partial X_i} + a_j\;\frac{\partial U_i}{\partial X_j} + a_k\,\frac{\partial U_i}{\partial X_k}\right] = \frac{2}{3}\,\delta\,(U_i-V_i)A \tag{3.10}$$

where a_i and a_k are constants.

If $\alpha\delta K(U_i-V_i)$ is much larger than this term, we can neglect the non-linear term. The condition becomes if a_j and a_k are equal to one and all the derivatives are equal

$$2\delta(U_i-V_i)\,\frac{\partial U_i}{\partial X_i} << \alpha\delta K(U_i-V_i)$$

or since K is near one,

$$2\,\frac{\partial U_i}{\partial X_i} << \alpha \tag{3.11}$$

Since α is approximately 10^7 for a one micron particle in air, the velocity gradient must be extremely large to be significant. Of course for a 100μ particle or a somewhat smaller particle in water this term may be important. It is possible then to calculate a particle velocity error in the same manner as shown below by taking the local value of A and using it to form a new correction K.

$$K^{II} = K + \frac{2A}{3\alpha} \tag{3.12}$$

This approach has been taken by Tchen [4]. The second derivative term can be neglected if it is small compared to the others. Hinze compares it to the velocity gradient term which gives

$$\frac{V}{d^2\,\dfrac{\partial^2 U_i}{\partial X^2}} >>> 1, \tag{3.13}$$

where d is the particle diameter. Comparing it to the same term as the velocity gradient we find.

$$\frac{2}{3}\,\nu\delta\nabla^2 U_i \ll \alpha\delta K(U_i - V_i)$$

and we can define

$$K^{III} = K + \frac{2A}{3\alpha} - \frac{2\nu}{3\alpha}\frac{\nabla^2 U_i}{(U_i - V_i)}\,. \qquad (3.14)$$

From eq. 3.14 we see that

$$\frac{2\nu}{3\alpha}\frac{\nabla^2 U_i}{(U_i - V_i)} \ll 1 \qquad (3.15)$$

is the condition to be met. Typical numbers in air are $\nu = 0.2$, $\alpha = 10^7$, $(U_i - V_i) = 10^{-3}$; so $\nabla^2 U_i \ll 10^3$ which is not the general situation. We will examine the effect of a local correction considered as a constant using eq. 3.14 later.

Equation 3.9 can be written as a linear first order differential equation using K^{III} as follows:

$$\frac{dV_i}{dt} = \delta\,\frac{dU_i}{dt} + \alpha\delta K^{III}(U_i - V_i) + \delta\left(\frac{3\alpha}{\pi}\right)^{\frac{1}{2}} \int_{-\infty}^{t} \frac{\frac{d}{d\tau}(U_i - V_i)}{\sqrt{t-\tau}}\,d\tau \qquad (3.16)$$

If the Basset term is dropped and $K^{III} = 1$, the equation becomes:

$$\frac{dV}{dt} + \alpha\delta V = \alpha\delta U + \delta\,\frac{dU}{dt} \qquad (3.17)$$

The Fourier transform of the solution is

$$\tilde{V} = \frac{\alpha + i\omega}{\alpha + i\,\frac{\omega}{\delta}}\,\tilde{U} \qquad (3.18)$$

We follow the procedure given by Soo [2] which was developed by Tchen [4] and Chao [32]. Multiplying eq. 3.18 by the complex conjugates of each side gives

$$\frac{\tilde{V}\tilde{V}^*}{\tilde{U}\tilde{U}^*} = \frac{(\frac{\omega}{\alpha}^2) + 1}{\frac{1}{\delta^2}(\frac{\omega}{\alpha})^2 + 1} \qquad (3.19)$$

which is the square of the amplitude ratio for the frequency, ω. For the particle the energy spectrum density function is introduced so that

$$\overline{V}^2 f_p(\omega) = \lim_{T\to\infty} \frac{\tilde{V}^*\tilde{V}}{2\pi T}\,. \qquad (3.20)$$

Integration with respect to ω gives

$$\overline{V^2} = \overline{U^2}\int_0^\infty \frac{(\frac{\omega}{\alpha})^2 + 1}{\frac{1}{\delta^2}\,(\frac{\omega}{\alpha})^2 + 1}\, f\,(\omega)\; d\omega \qquad (3.21)$$

and

$$\frac{f_p}{f} = \frac{\overline{U^2}}{\overline{V^2}}\;\frac{(\frac{\omega}{\alpha})^2 + 1}{\frac{1}{\delta^2}\,(\frac{\omega}{\alpha})^2 + 1}\,, \qquad (3.22)$$

where f is the energy spectrum density function for the fluid.

The same problem can be solved for the relative velocity and if the Basset term is included. Details are given by Soo. Inclusion of the Basset term or corrections to the drag coefficient have the same effect as decreasing the particle size. Therefore, the particles follow the flow better than would be indicated by eq. 3.21.

Calculations have been made by Hjelmfelt and Mockros [33] for the amplitude at a given frequency. Results are similar to the acoustic results given in section II. Figure 3.1 shows the effect of particle size on the amplitude ratio for particles in air when all terms are included in the equation but only Stokes drag is considered. We have chosen cases of pipe flow and free jet flow where the frequency spectra is known except for the high frequency range for our calculations. The results given in the next sections are for particle-fluid relationships for the fluctuating component of the turbulent velocities.

A list of the equations to be used in the subsequent discussion is given below so easy reference can be made to them.

Accoustic:

A-I $$\frac{\overline{V_o^2}}{\overline{U_o^2}} = \int_0^\infty \frac{f(\omega)d\omega}{1+a^2\omega^2} .$$

A-II $$\frac{\overline{V^2}_{r_o}}{\overline{U^2}_o} = 1 - \frac{\overline{V^2}_o}{\overline{U^2}_o}$$

$$a = \frac{2r^2\rho_p}{9\mu}$$

<u>Approximate Turbulent:</u>

T-I $$\frac{\overline{V^2}}{\overline{U^2}} = \int_0^\infty \frac{(\frac{\omega}{\alpha})^2 + 1}{\frac{1}{\delta^2}(\frac{\omega}{\alpha})^2 + 1} f(\omega)\, d\omega$$

T-II $$\frac{\overline{V^2}_r}{\overline{U^2}} = \int_0^\infty \frac{(\frac{1-\delta}{\delta})^2(\frac{\omega}{\alpha})^2}{\frac{1}{\delta^2}(\frac{\omega}{\alpha})^2 + 1} f(\omega) d\omega$$

Turbulent with Basset force.

T-III $$\frac{\overline{V^2}}{\overline{U^2}} = \int_0^\infty \frac{\Omega^{(1)}}{\Omega^{(2)}} f(\omega) d\omega$$

T-IV $$\frac{\overline{V^2}_r}{\overline{U^2}} = \int_0^\infty \frac{\Omega_R^{(1)}}{\Omega^{(2)}} f(\omega) d\omega$$

$$\Omega^{(1)} = (\frac{\omega}{\alpha})^2 + \sqrt{6}\,(\frac{\omega}{\alpha})^{3/2} + 3(\frac{\omega}{\alpha}) + \sqrt{6}\,(\frac{\omega}{\alpha})^{\frac{1}{2}} + 1$$

$$\Omega^{(2)} = \frac{1}{\delta^2}\left(\frac{\omega}{\alpha}\right)^2 + \frac{\sqrt{6}}{\delta}\left(\frac{\omega}{\alpha}\right)^{3/2} + 3\left(\frac{\omega}{\alpha}\right) + \sqrt{6}\left(\frac{\omega}{\alpha}\right)^{1/2} + 1$$

$$\Omega_R^{(1)} = \left(\frac{1-\delta}{\delta}\right)^2 \left(\frac{\omega}{\alpha}\right)^2$$

Turbulent with Basset force and drag coefficient $(24/N_{Re})K$.

T-V Replace the last two terms in $\Omega^{(2)}$ and $\Omega^{(1)}$ with

$$\sqrt{6}\, K \left(\frac{\omega}{\alpha}\right)^{1/2} + K^2.$$

All velocities in the above are fluctuations from the mean.

Figure 3.1 shows the amplitude function $\Omega^{(1)}/\Omega^{(2)}$ as a function of frequency and particle size for air as the fluid. Errors of over 1% exist when the frequency is over 6kH$_2$ for a one micron particle and for frequencies considerably less as the particle size increases. The effect of changing the parameter K is shown in Figure 3.2. As K is increased the drag increases and the amplitude function increases. This means that the relative velocity lag is reduced.

Fortunately in a turbulent field most of the energy is concentrated in low frequency oscillations. That is $f(\omega)$ drops off rapidly as frequency is increased. We examine the cases of the free jet and the center of fully developed pipe flow in the following subsections. The assumptions that the particle and fluid diffusivities are the same (long diffusion time) and no particle-particle interactions are retained.

A. Application of Single Particle Analysis to Turbulent Jets

Based on J. C. Laurence's [34] measurements in the mixing region of a free jet, the spectral density function can be represented by f_{max}, f_w

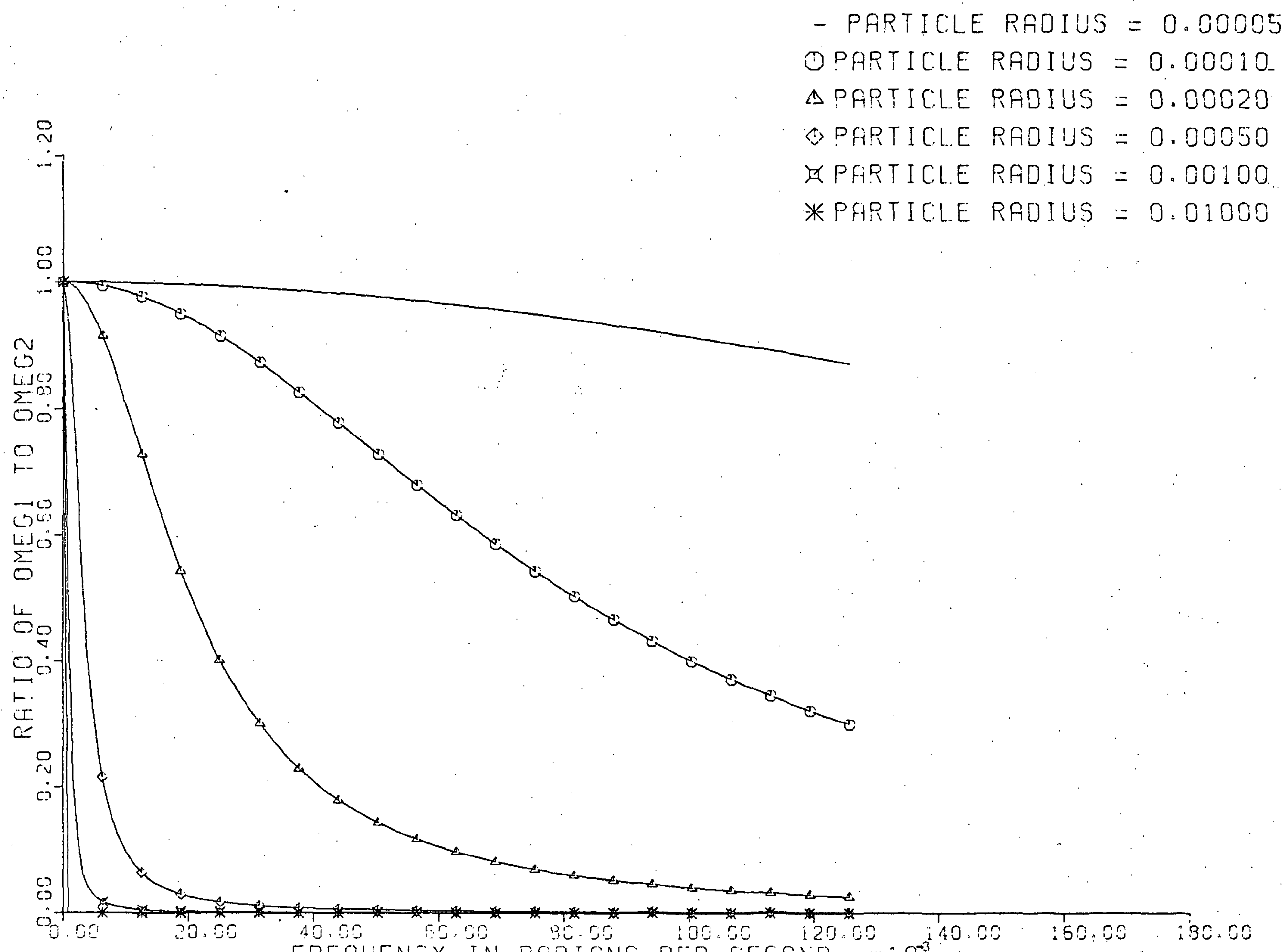
- PARTICLE RADIUS = 0.00005
PARTICLE RADIUS = 0.00010
PARTICLE RADIUS = 0.00020
PARTICLE RADIUS = 0.00050
PARTICLE RADIUS = 0.00100
PARTICLE RADIUS = 0.01000
RATIO OF OMEG1 TO OMEG2
0.00
0.20
0.40
0.60
0.80
1.00
1.20
0.00
20.00
40.00
60.00
80.00
100.00
120.00
140.00
160.00
180.00
FREQUENCY IN RADIANS PER SECOND *10^-3

FIGURE 3.1

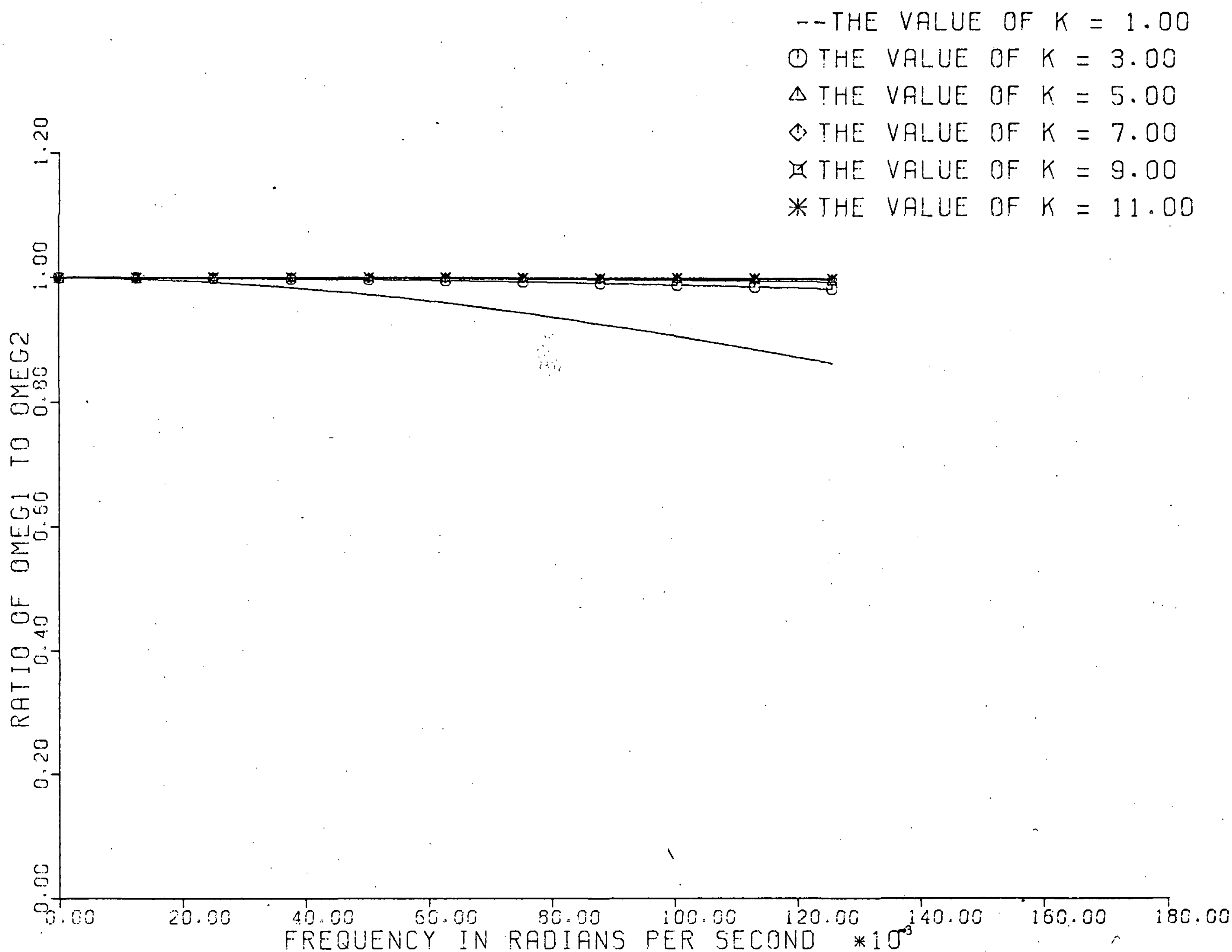
--THE VALUE OF K = 1.00
THE VALUE OF K = 3.00
THE VALUE OF K = 5.00
THE VALUE OF K = 7.00
THE VALUE OF K = 9.00
THE VALUE OF K = 11.00
RATIO OF OMEG1 TO OMEG2
0.00
0.20
0.40
0.60
0.80
1.00
1.20
0.00
20.00
40.00
60.00
80.00
100.00
120.00
140.00
160.00
180.00
FREQUENCY IN RADIANS PER SECOND $*10^3$

FIGURE 3.2

and a decay slope of -2 on a log-log plot of $f(\omega)$ vs ω as shown in Fig. 3.3. Using Equation T-IV extensive calculations showed the results were sensitive only to f_u when particle diameter and density were held constant.

The density function decay as the inverse square cannot exist beyond some upper limit frequency. Most references on turbulence give a change from a minus 5/3 slope to a minus 7 slope for isotropic turbulence at some high frequency. That is at some frequency of turbulence all the energy should be dissipated by the viscous forces. If this frequency is taken as 20 kHz and we neglect everything beyond 20 kHz, calculations can be made giving mean square differences between particles and fluid using the equations listed. For a one micron diameter particle with a density of one gram per cubic centimeter in an air jet mixing region with f_u = 2000 Hz the results are:

Equation	Result
A-I	.991
T-I	1.000
T-III	.990
A-II	.009
T-II	.009
T-IV	.008

Further calculations using formula T-IV are summarized in Figs. 3.4 and 3.5, Figure 3.4 shows the effect of particle density for different f_u and particle size. Figure 3.5 shows the effect of particle size when particle density is held constant at one gram per cubic centimeter.

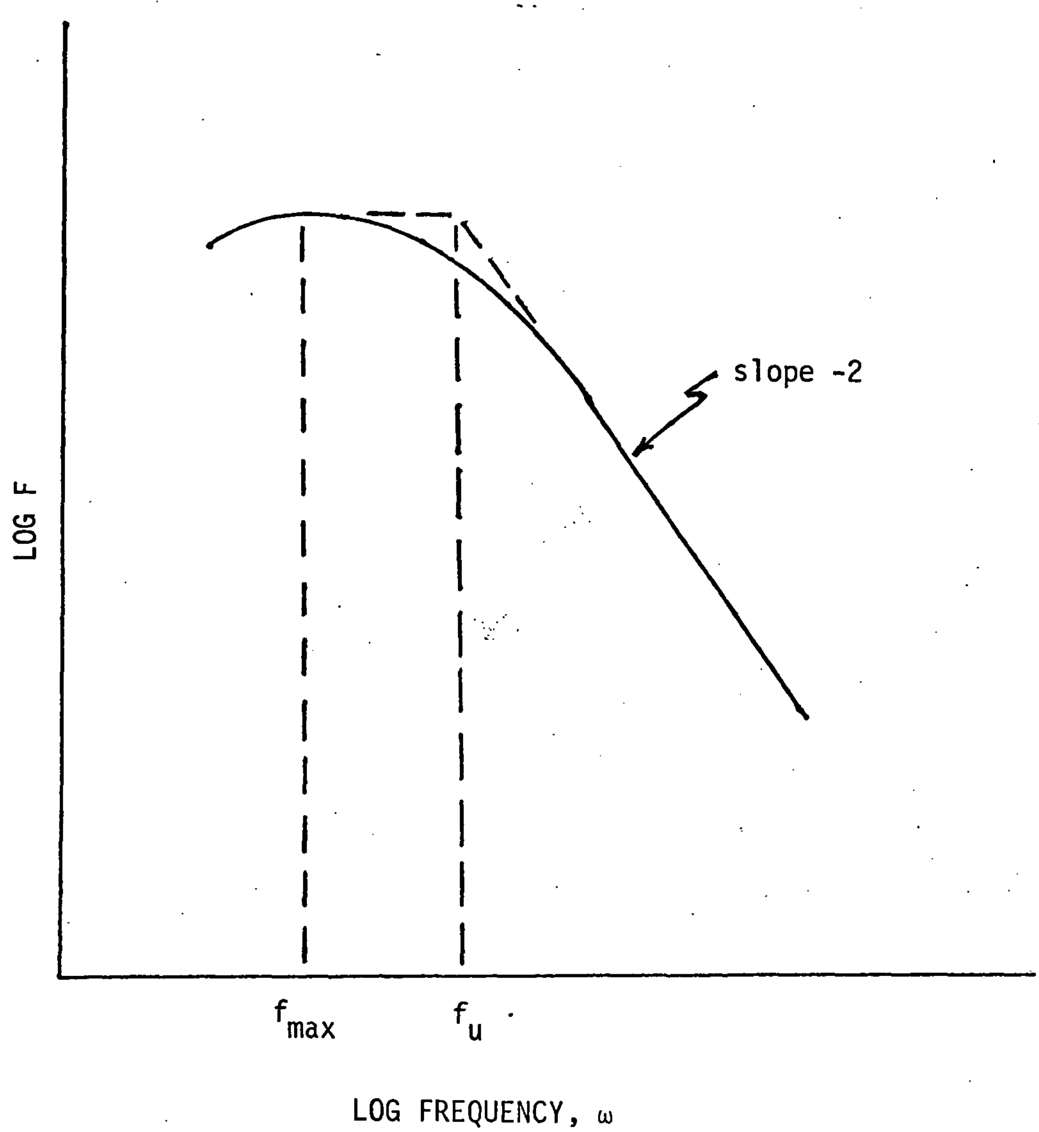

Figure 3.3 Turbulent Jet Frequency Spectra

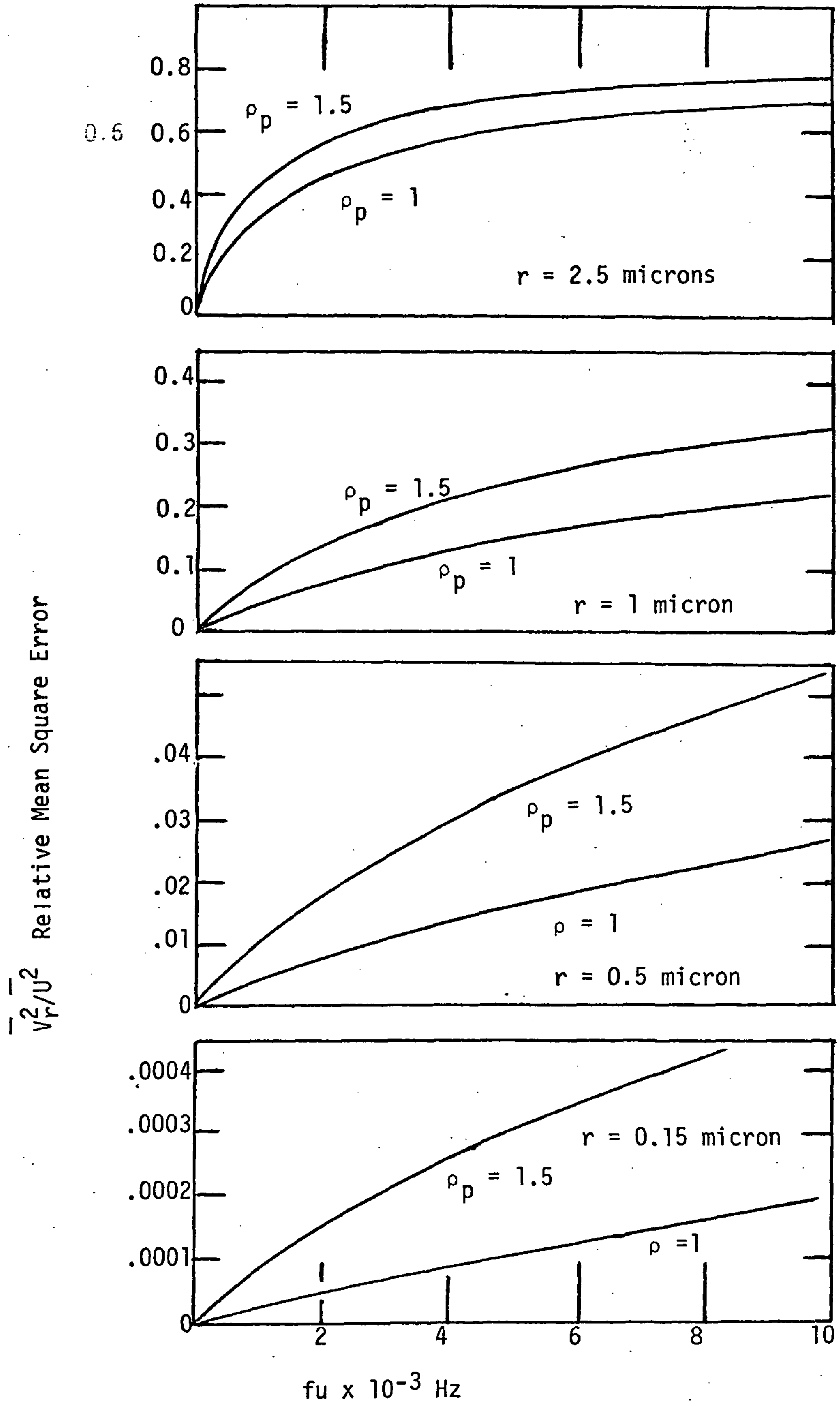

Figure 3.4 Particle Density Effect on Velocity Lag.

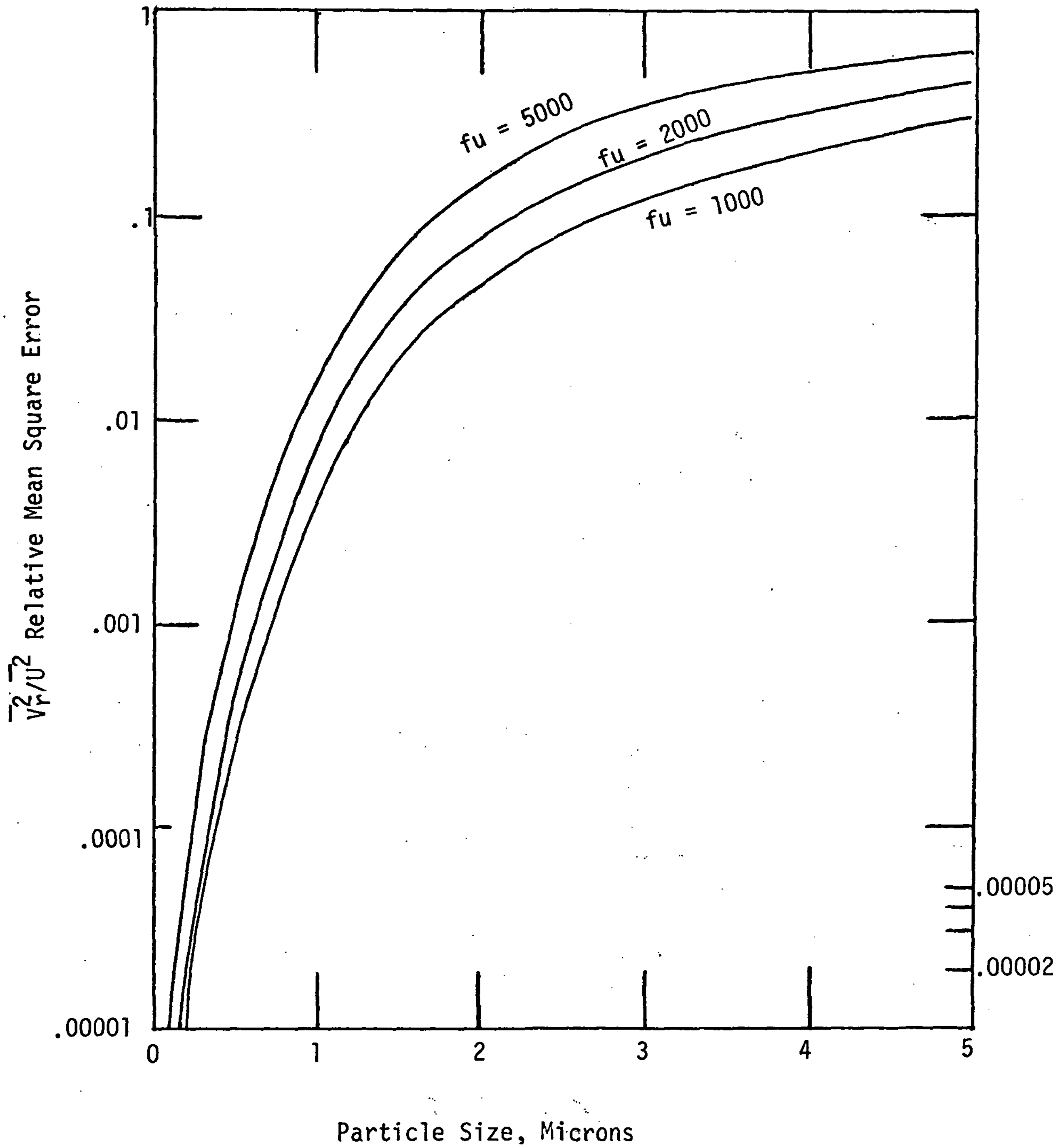

Figure 3.5 Effect of Upper Cut Off Frequency

In each case the frequency spectrum density function was taken from Laurence's equation.

$$E(f_{max}, fu, \omega) = \frac{(1 + k_1)(\frac{\omega}{f^*})^2}{(4f^*)[1 + (\frac{\omega}{f^*})^2][k_1 + (\frac{f}{f^*})^2]}$$

$$k_1 = \left(\frac{f_{max}}{2\pi f^*}\right)^2$$

$$f^* = \frac{fu}{2}\left[1 + \sqrt{1 - \left(\frac{f_{max}}{\pi fu}\right)^2}\right]$$

The integration was carried out using 50 points and the trapezoidal rule between 0 and 20 kHz. The $f(\omega)$ function in equations is the above E function divided by

$\int_0^{20\ \text{kHz}} E\, d\omega$ to normalize the function.

A simpler analysis can be made using E a linear function of ω^{-2}. Figures 3.6 and 3.7 show the ratios of particle mean or relative velocity fluctuations to the fluid fluctuation for selected particle sizes from one micron diameter to 200 micron diameter. Air is taken as the fluid at room temperature.

The effects of non Stokes drag, rarefaction, compressibility and inertia can be included in the equation of motion by letting

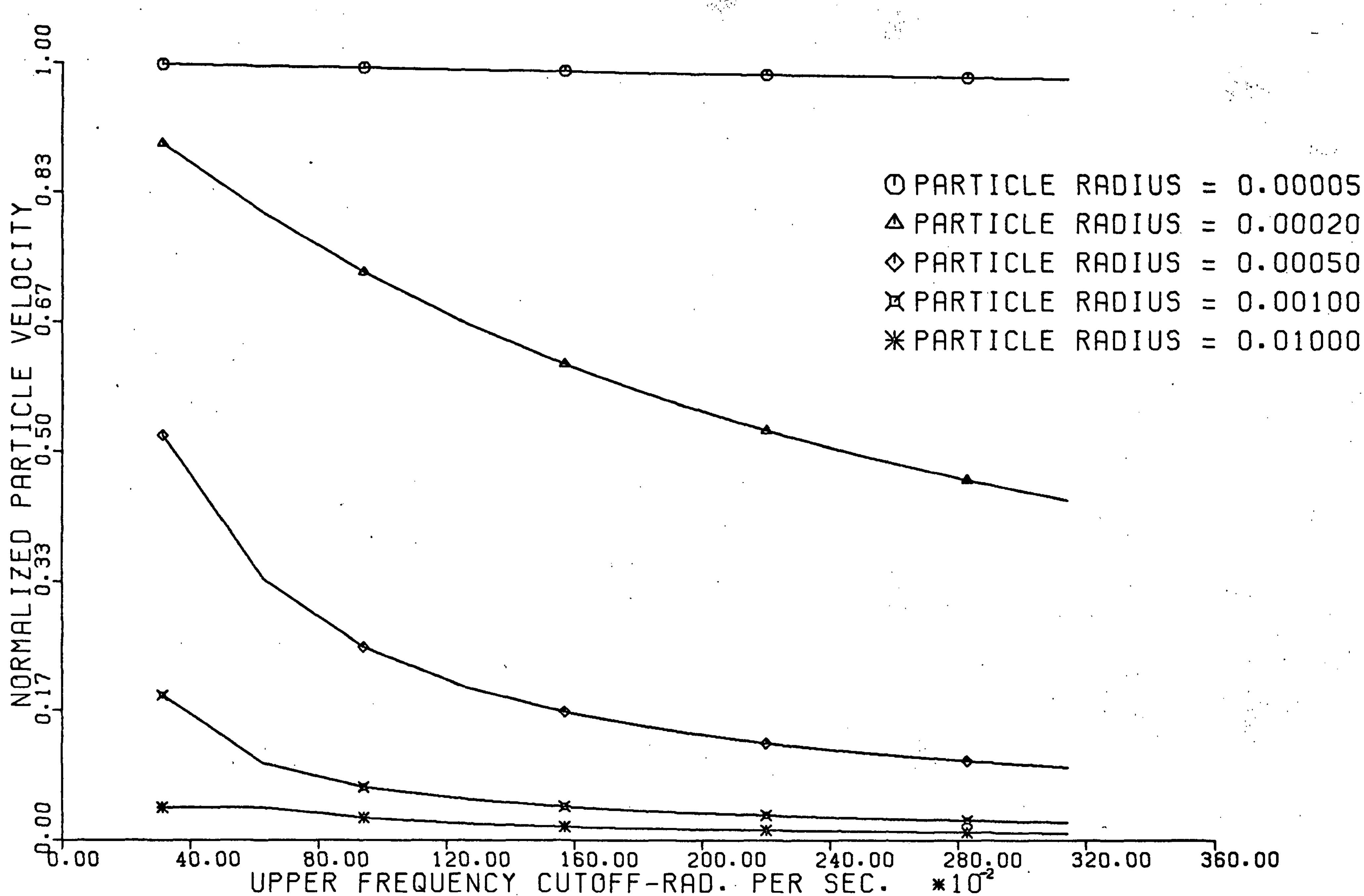

FREE-JET SITUTATION

FIGURE 3.6

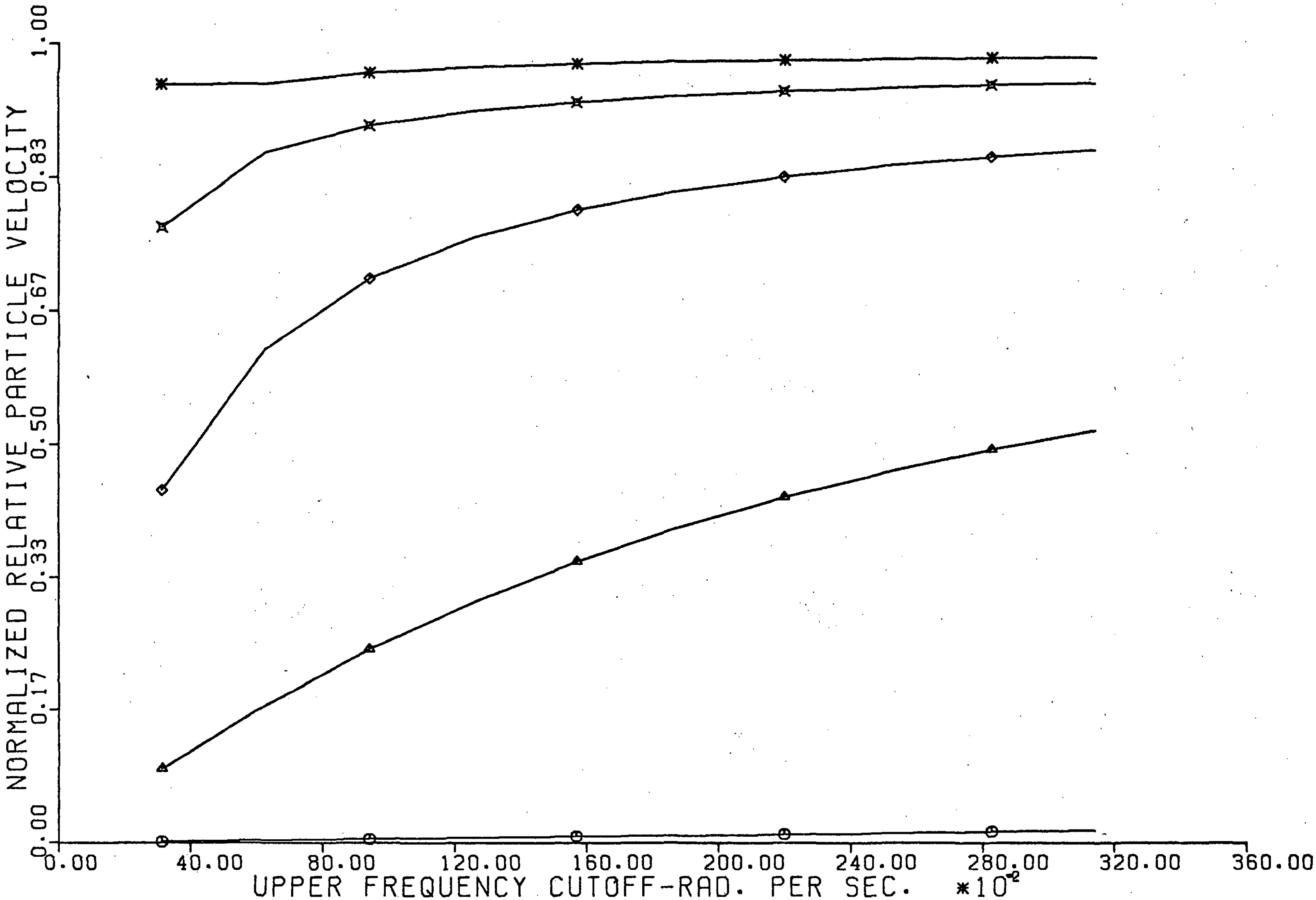

FREE-JET SITUTATION

FIGURE 3.7

$$K = \frac{(1 + 0.15N_{Re}^{0.687})(1 + \exp(-0.427/M^{4.63} - 3.0/N_{Re}^{0.88}))}{1 + \frac{M}{N_{Re}}(A + B\exp(-1.25N_{Re}/M))}$$

where the Reynolds number, N_{Re}, and the Mach Number, M, are for the difference velocity between the fluid and particle. The constants A and B are 3.82 and 1.28 respectively at Mach numbers sufficiently high, but may be lower for lower Mach numbers. The equation above is derived by Carlson and Hoglund [27].

For a one micron diameter particle with a density of one gram per cubic centimeter moving in air at room temperature, the following results were obtained:

Mach No. of fluid	Mean square ratio of velocities	Mean square relative velocity to fluid velocity	Particle Reynolds Number	Particle Mach Number
0.1	.9878	.0096*	.218	.0098
0.3	.9889	.0087*	.623	.0281
0.5	.9897	.0082*	1.003	.0452
1.0	.9909	.0072	1.883	.0848
2.0	.9924	.0061	3.454	.1556

In the table the complete equation was used although the rarefaction correction in the denominator is not valid for the starred points. In general for this particle size at a cut-off frequency of two KHz as used in the calculations there is no significant change. All of the conditions, however, fall in the slip flow regime and not the continuum regime.

B. Single Particle in Pipe Flow

A similar analysis can be made for fully developed turbulent pipe flow. For the frequency spectra Laufer's data [35] can be used. The upper cut off frequency is now a function of Reynolds number or average velocity. If the minus second power decay of the frequency spectra can be used, the curves for the free jet would also be valid for the drag corrections. From Laufer's curve at the centerline of the one dimensional spectra

$$0.28\ U_{x_1\ max} \cong fu$$

where fu is in radians per second and $U_{x_1\ max}$ in cm./sec. Laufers curve is for a Reynolds number of 5 x 10^5, however, and may not be representative of lower Reynolds numbers.

C. Experimental Studies of Turbulent Velocities of Small Particles

A summary of the few experimental measurements on turbulence intensities in particle-fluid flows is given by Reddy and Pei [36]. Other studies discussed in Part IV of this report are indirect in that measurements were made on concentration fluctuations and not velocities. The velocity studies were made photographically using particles greater than 100 microns. Reddy and Pei conclude that "the particle turbulence components can be correlated principally with the fluid turbulence." It is difficult to justify this statement based on the calculations in this report. Only the slowly varying large scale motions follow the flow and therefore the turbulence intensities of the particle and the fluid check closely. However, it is impossible to measure the high frequency turbulence components by measuring velocities of particles larger than one micron.

A study in liquids using 0.5 micron particles was recently reported by Corino and Brodkey [37]. They were successful in measuring particle velocity fluctuations near the wall of a pipe at Reynolds numbers up to 50,000. Velocity gradients as high as 10^4 sec.$^{-1}$ could be determined.

Soo [2] reviews other experiments but the interaction of the solid particles with the wall has been a problem. Min [38] indicates that the spread of velocities after collision with the wall must be considered and not confused with the turbulence of the main stream. In section I of this report the time decay was seen to influence the relative mean velocity. Measurements of turbulence from velocities of large particles would consist of large effects due to these adjustments following collisions.

IV. OTHER CONSIDERATIONS IN PARTICLE-FLUID FLOWS

Two assumptions of the previous section are not substantiated by experiments. These are the assumption that particle and fluid diffusivities are the same, and the neglect of particle-particle collisions. Extensive theoretical and experimental investigations have appeared in the literature on both problems, but it is not possible to predict or measure the effects in most real situations.

Soo [2] derives the eddy diffusivity for the particle from the mean square displacement. If the mean square displacement is related to the Lagrangian velocity auto correction coefficient, R(t), the result is

$$D_p(t) = \overline{V}^2 \int_0^t R_p(\tau) d\tau \tag{4.1}$$

The fluid eddy diffusivity similarly is

$$D = \overline{U}^2 \int_0^t R(\tau)\, d\tau \tag{4.2}$$

Friedlander [29] explains that $R(\tau)$ is Lagrangian only for small particles and may be between the Eulerian and Lagrangian correlations for the real case. The ratios of particle to fluid eddy diffusivity become

$$\frac{D_p}{D} = \frac{\overline{V}^2}{\overline{U}^2} \quad \text{for short times}$$

and $$\frac{D_p}{D} = 1 \quad \text{for long times}$$

Both Soo and Friedlander give results for an assumed Lagrangian coefficient. In the previous section the assumption was made that $D_p/D = 1$, but studies by Lumley [28] and others show that this is not true. To account for the difference we must relax the assumption that a particle remains always with the same fluid element. Soo gives a review of calculations to correct the eddy diffusivity for some practical cases. If the particles are below one micron in diameter, however, the assumptions of section III appear to be valid when sufficient time is given for the particle-fluid system to equilibrate. Collisions with walls or other particles, velocity gradients or coalescence will affect this time period.

Some of the first work in the field of particle-particle interactions was published by Smoluchowski in 1916. He developed an infinite set of simultaneous differential equations to describe the interactions and growth of flocs. His results may be written in condensed form as

$$\frac{dN_k}{dt} = \frac{2}{3}\frac{dU}{dZ}\left[\sum_{\substack{i=1\\j=k-i}}^{k-1} N_i N_j (R_i+R_j)^3 - 2N_k \sum_{i=1}^{\infty} N_k (R_i+R_k)^3\right] \tag{4.3}$$

where dN/dt is the rate of change of the number of particles of the indicated size, dU/dZ is the velocity gradient, N is the number of particles of an indicated size, and R is the radius of the particles. It is not possible to solve this set of equations in a closed form for real cases; however, with the advent of large computer systems approximate solutions have been made. [39, 40].

A program is available from R. S. Gremmell [41] in which the growth, breakup, and steady state size of flocs in laminar flow are simulated as a function of the maximum floc size, the breakup floc sizes, the velocity gradient, and the initial concentration of the suspension. This type of simulation is very helpful if the necessary variables are known for a particular system. Such simulations are, of course, only useful if the particles tend to floc or coagulate.

The availability of sophisticated equipment has made experimental studies of single particle interactions possible. In the study of rigid spheres, Mason and others [42] discovered a repeatable pattern of approach, interaction, and separation. The spheres approach each other rectilinearly in a path parallel to the x-axis (i.e. axis parallel to the flow). Although they never come into true physical contact the two approaching spheres form a doublet which rotates with a constant angular velocity of

$$\omega = \frac{G}{2}$$

where G is the velocity gradient in the fluid. The doublet rotates about an axis perpendicular to the planes of shear, and in the case of rigid spheres the doublet only rotates 180°. The separation is a mirror image of the approach because of the 180° rotation before separation. Deformable spheres do not separate after the first half cycle but may rotate for several full cycles before coalescing or separating. They will coalesce only if the van der Waals forces are strong enough to displace the intervening liquid. [43]

The tubular pinch effect is a fluid induced particle disturbance found only in tubular Poiseuille flow and not in Couette flow. The tubular pinch effect is essentially the tendency for rigid or deformable bodies to migrate under certain conditions toward a radial position of distance r from the center of the tube. The particles closer to the center of the tube migrate inward. This effect is apparently not encountered in turbulent flows although the forces causing the phenomenum may be important in the analysis given in the previous section.

Karnis and Mason [44] have obtained an expression for the radial position, r, of a liquid drop as a function of time, t, and indicated that a rigid sphere follows this behavior very closely. Their result is given as

$$\frac{R_o}{r} + 2\,\ln\left(\frac{r}{R_o}\right) - \frac{r}{R_o} = \left(\frac{k^2 b^4 \eta_o t}{\gamma R_o}\right) \frac{33(54p^2+102p+54)(19p+16)}{4480(p+1)^3} + A \qquad (4.4)$$

where R_o is the radius of the tube, k is given as $4Q/(R_o^4)$, Q being the volumetric flow rate, b is the original radius of the undeformed drop, η_o is the viscosity of the suspending fluid, γ is the interfacial tension, p is the viscosity ratio of the suspended to the suspending phase, and

$$A = \frac{R_o}{r_o} + 2\,\ln\left(\frac{r_o}{R_o}\right) - \frac{r_o}{R_o}\,,$$

where r_o is the initial position of the drop. The actual migration rate in some cases has been found to be lower than that predicted by equation 4.4.

Takano, Goldsmith, and Mason [45] investigated the effect of a sine wave fluid disturbance superimposed on the steady state flow. Although their work is not complete, they have come to some qualitative conclusions. The migration rates and equilibrium positions for a given suspension depend on a dimensionless parameter, α, as well as the flow rate. The parameter

$$\alpha = R_o\left(\frac{\omega\rho_o}{\eta_o}\right)^{\frac{1}{2}},$$

where R_o and η_o are the same as before, ω is the angular frequency of oscillation, and ρ_o is the density of the suspending fluid. This parameter was used in the analysis of both rigid and deformable spheres.

In experiments made with polystyrene spheres, the initial stages of oscillatory flow, $\alpha<5$, revealed an increased migration rate over that of steady state Poiseuille flow. The particles collided in approximately the same manner as observed in the former particle interaction studies in steady state laminar flow. As α became larger than ten, more than one migration or equilibrium position was noted. Some of these positions, defined as radii where dr/dt for the particle equaled zero, were found to be quasi-stable. The number of these positions increased with increasing α, and it would be expected that at sufficiently high α the number of these quasi-stable positions would destroy any noticeable migration caused by the tubular pinch effect.

In a study concerned with the agglomeration of aerosols induced by high energy sound waves St. Clair [46] listed three fluid effects on particle movements. These were convibrational, hydrodynamic and radiation pressure.

Another analysis by Shaffman and Turner [47] concerned the collision of liquid droplets in turbulent clouds. Assuming isotropic turbulence, the collisions of the drops are attributed to two main sources: (1) collisions due to the motions of the droplets in (within) the air, (2) collisions due to motions of the droplets relative to the air (i.e. inertial effects). The two effects are discussed separately; the two effects may be calculated separately and then added together.

The collisions caused by the drops moving with the fluid are discussed assuming spherical droplets with a sphere of influence, R, equal to the sum of the radii of two particles, $r_1 + r_2$. With a radial particle velocity of w(r), some fluid relations can be used to transform w(r) into fluid properties. After the transformation, the number of collisions, N, between two population concentrations, n_1 and n_2, is

$$N = 1.3\ n_1 n_2\ (r_1 + r_2)\ (\frac{\varepsilon}{\gamma})\ , \qquad (4.5)$$

where ε is the rate of energy dissipation per unit mass, and γ is the kinematic viscosity.

In order to obtain the total effect of the collisions, the collision rate is substituted into the Smoluchowski equation.

In dealing with the second part of the problem, that of droplet motions relative to the air as causes of collisions, a probability function $P(\underline{\overline{w}})$ for the relative velocity of the particles is assumed and the collision rate thus obtained is

$$N = \pi R^2\ n_1 n_2 \int \underline{\overline{\omega}}\ P(\underline{\overline{\omega}}) d\underline{\overline{\omega}} \qquad (4.6)$$

By introducing a collision efficiency a quantitative prediction of droplet formation in turbulent clouds can be obtained.

Another theoretical development of turbulent coagulation was made by H. C. Frish [48]. Homogenous and isotropic turbulence was considered in a fluid macroscopically at rest. In order to describe such turbulence, a factor of turbulent diffusion, n* is defined as

$$N^*(t) = \bar{\nu}^2 \int_0^t R_h\ (\alpha) d\alpha + D \tag{4.7}$$

where D is the molecular diffusion coefficient, R_h is the Lagrangian correlation coefficient of the field of turbulence and $\bar{\nu}^2$ is the variance of the turbulent velocities. This definition is augmented with the assumption that the probability density for the particle is Gaussian and which gives

$$N^*_{1,2}(t) = N^*_1(t) + N^*_2(t) \tag{4.8}$$

He next makes the common assumption that a particle fixed in space has a sphere of influence of $R_{1,2} = r_1 + r_2$, where r_1 and r_2 are the respective radii of two colliding particles. He considers the collision frequency to be one. Using the above conditions an expression for the rate of formation of a particle of the size i+k can be written. Then the concentration distribution can be calculated.

Becker, Hottel, and Williams, optically measured the concentration fluctuations in a particle-fluid nozzle flow [49]. Although they assumed the velocity and concentration fluctuations were alike, the results showed the characteristic difference in the diffusion broadening. It is apparent that little data are available to properly check the differences between particle and fluid velocity fluctuations at high rates of change.

V. CONCLUSIONS

Small particles can be used to measure the fluid velocity motions except under conditions of high frequency fluctuations. At high velocities, in supersonic flow and for detailed analyses of turbulence, all particle-fluid-instrument interactions must be considered. Both more theoretical correlations for these conditions and experimental measurements under more ideal conditions are needed to determine the exact limits of the Laser-Doppler Flowmeter and the particle lag corrections.

VI. LITERATURE CITED

1. Fuchs, N. A., "The Mechanics of Aerosols", Macmillan Co., New York 1964.

2. Soo, S. L., "Fluid Dynamics of Multiphase Systems," Blaesdell Publishing Co., Waltham, Mass. 1967.

3. Basset, A. B., "A Treatise on Hydrodynamics", Vol. 2, Dover Publications New York, 1961, Chapter 22.

4. Tchen, C. M., "Mean Value and Correlation Problems Connected with the Motion of Small Particles Suspended in a Turbulent Fluid," PhD Thesis, Delft, 1947.

5. Hinze, J. O., "Turbulence", McGraw-Hill Book Company, Inc., New York, 1959.

6. Reddy, K.V.S., M. C. Van Wijk and D. C. T. Pei, "Stereophotogrammetry in Particle-Flow Investigation," Canadian Journal of Chemical Engineering, 47, 85 (1969).

7. Hughes R. R. and E. R. Gilliland, "The Mechanics of Drops," Chemical Engineering Progress, 48, 497 (1952).

8. Corrsin, S., and M. S. Uberoi, NACA Tech. Note 1965, 1949.

9. Gilbert, M., L. Davis and D. Altman, "Velocity Lag of Particles in Linearly Accelerated Combustion Gases," Jet Propulstion, 25, 26 (1955).

10. James, R. N., W. R. Babcock and H. S. Seifert, "Application of a Laser-Doppler Technique to the Measurement of Particle Velocity in Gas Particle Two Phase Flow," SUDAAR No. 265, Dept. of Aeronautics and Astronautics, Stanford University, Stanford, California, May 1966.

11. McCarthy, H. E. and J. H. Olson, "Turbulent Flow of Gas Solids Suspensions," I&EC Fundamentals, 7, 471 (1968).

12. Torobin, L. B. and Gauvin Wtt, AIChE J., 7, 406 (1961), AIChE J., 7, 615 (1961), Can. J. Chem Eng 37, 1959 (1959), Can. J. Chem Eng, 38, 189 (1960).

13. Morse, H. L., B. J. Tullis, H. S. Seifert, and Wayne Babcock, "Development of a Laser-Doppler Particle. Sensor for the Measurement of Velocities in Rocket Exhausts," J. Spacecraft and Rockets, 6, 264 (1969).

14. James, R. N., W. R. Babcock and H. S. Seifert, "A Laser-Doppler Technique for the Measurement of Particle Velocity," AIAA Journal 6, 160 (1968).

15. Fulmer, R. D. and D. P. Wirtz, "Measurement of Individual Particle Velocities in a Simulated Rocket Exhaust," AIAA paper 65-11 and AIAA J. 3, 1506 (1965).

16. Afanasev, E. F. and V. N. Nikolaevskii, "On the Development of Asymmetric Hydrodynamics of a Suspension With Rotating Solid Particles," Problems of Hydrodynamics and Continuum Mechanics, SIAM, Philadelphia, 1969.

17. Hoerner, S. F., Fluid Dynamic Drag, Horner, Midland Park, N. J. (1958).

18. Rubinow, S. I. and J. B. Keller, J. Fluid Mech. 11, 477 (1961).

19. Eichhorn, R. and S. Small, J. Fluid Mech. 20, 513 (1964).

20. Saffman, P. G., J. Fluid Mech. 22, 385 (1965).

21. Kondic, N. N., "Lateral Motion of Individual Particles in Channel Flow - Effect of Diffusion and Interaction Forces: Part 1 - Particle Behavior as a Function of Systematic Motion," ASME 69-HT-32.

22. Lamb, H., "Hydrodynamics," Dover Publications, New York, 1945.

23. Landau, L. D. and E. M. Lifshitz, "Fluid Mechanics," Pergamon Press, London, 1959.

24. Rosensweig, R. E., Hoyt C. Hottel and G. C. Williams, "Smoke-scattered Light Measurement of Turbulent Concentration Fluctuations," Chemical Engineering Science 15, 111 (1961).

25. Konig, W., Ann. Physik 42, 353 (1891).

26. Torobin, L. B. and W. H. Gaurin, Can J. Chem. Eng. 37, 129, 167, 224, (1959), Can. J. Chem. Eng. 38, 142, 189 (1960), and Can. J. Chem. Eng. 39, 113 (1961).

27. Carlson, D. J. and R. F. Hoglund, "Particle Drag and Heat Transfer in Rocket Nozzles," AIAA Journal 2, 1980 (1964).

28. Lumley, J. L., "Some Problems Connected With the Motion of Small Particles in Turbulent Fluid," Dissertation, Johns Hopkins University, Baltimore, Maryland, 1957.

29. Friedlander, S. K., AIChE Journal 3, 381 (1957).

30. Brodkey, R. S., "The Phenomena of Fluid Motions," Chap. 18, Addison-Wesley Publishing Co., 1967.

31. Corrsin and J. Lumley, Appl. Sci Res 6A, 114 (1956).

32. Chao, B. T., Osteneichisches Ingenieur-Archiv 18, 7 (1964).

33. Hjelmfelt, A. T. and C. F. Mockres, "Motion of Discrete Particles in a Turbulent Fluid," Appl. Sci Res 16, 149 (1966).

34. Laurence, J. C.,"Intensity, Scale, and Spectra of Turbulence in Mixing Region of Free Subsonic Jet," NACA Report 1292.

35. Laufer, J., NACA Tech Report 1147 (1954).

36. Reddy, K. V. S. and D. C. T. Pei, I&EC Fund. 8, 490 (1969).

37. Corino, E. R. and R. S. Brodkey, J. Fluid Mech. 37, 1 (1969).

38. Min, K, J. Appl. Phys. 38, 564 (1967).

39. Fair, G. M. and R. S. Gremmell, J. Colloid Science 19, 360 (1964).

40. Vold, M. J., J. Colloid Science 18, 684 (1963).

41. Gremmel, R. S., "Some Aspects of Orthokenetic Flocaelation, PhD Thesis, Cambridge, 1963.

42. Mason, S. G. and R. St. J. Manley, Canadian J. of Chemistry 33, 763 (1955).

43. Mason, S. G. and W. Bartok, J. Colloid Science 14, 25 (1959).

44. Mason, S. G. and A. Karnis, J. of Colloid and Interface Science 24, 165 (1967).

45. Takano, M., H. L. Goldsmith and S. G. Mason, J Colloid Interface Science 27, 254 (1968).

46. St. Clair, H., Industrial and Engineering Chemistry 41, 2434 (1949).

47. Saffman, P. G. and J. F. Turner, J. Fluid Mechanics 1, 16 (1956).

48. Frish, H. L., J. Phys. Chem. 60,463 (1956).

49. Becker, H. A., H. C. Hottel and G. C. Williams, J. Fluid Mech 30, 259 (1967).